

RADIO EFFICIENCY OF PULSARS

ANDRZEJ SZARY^{1,2}, BING ZHANG^{3,2}, GEORGE I. MELIKIDZE^{1,4}, JANUSZ GIL¹ AND REN-XIN XU²*Draft version February 4, 2014*

ABSTRACT

We investigate radio emission efficiency ξ of pulsars and report a near linear inverse correlation between ξ and the spindown power \dot{E} , as well as a near linear correlation between ξ and pulsar age τ . This is a consequence of very weak, if any, dependences of radio luminosity L on pulsar period P and period derivative \dot{P} , in contrast to X-ray or γ -ray emission luminosities. The analysis of radio fluxes suggests that these correlations are not due to a selection effect, but are intrinsic to the pulsar radio emission physics. We have found that, although with a large variance, the radio luminosity of pulsars is $\langle L \rangle \approx 10^{29}$ erg/s, regardless of the position in the $P - \dot{P}$ diagram. Within such a picture, a model-independent statement can be made that the death line of radio pulsars corresponds to an upper limit in the efficiency of radio emission. If we introduce the maximum value for a radio efficiency into Monte Carlo-based population syntheses we can reproduce the observed sample using the random luminosity model. The Kolmogorov-Smirnov test on a synthetic flux distribution shows high probability of reproducing the observed distribution. Our results suggests that the plasma responsible for generating radio emission is produced under similar conditions regardless of pulsar age, dipolar magnetic field strength, and spin-down rate. The magnetic fields near the pulsar surface are likely dominated by crust-anchored magnetic anomalies, which do not significantly differ among pulsars, leading to similar conditions for generating electron-positron pairs necessary to power radio emission.

Subject headings: pulsars: general

1. INTRODUCTION

Despite the fact that pulsars were discovered almost half a century ago, the emission mechanism of the pulsed radio emission remains unresolved. The challenge lies in the difficulty to identify the correct “coherent” mechanism (Melrose 2006) that can power radio emission with similar emission characteristics over about four orders of magnitude in rotation period P and up to eleven orders of magnitude in the rate of increase of pulsar periods $\dot{P} = dP/dt$. In this paper we perform a systematic analysis of radio emission efficiency for the current sample of pulsars⁵, in an effort to study the global radio emission properties and to constrain radio emission mechanism. In Section 2 we present the method to calculate radio luminosity L and radio emission efficiency ξ of pulsars. The dependences of both L and ξ on pulsar parameters are presented in Section 3. The results are summarized in Section 4 along with a discussion on the physical implications of the found correlations.

2. RADIO LUMINOSITY AND EFFICIENCY

2.1. Integrated radio luminosities

For a number of reasons a correct estimate of a pulsar’s radio luminosity is difficult (see e.g. Lorimer et al. 2004). A common practice is to assume that the intensity distribution along the observer’s line-of-sight cut through the emission region is representative for the entire emission beam. Then, the luminosity of a pulsar can be calculated as follows:

$$L = \frac{4\pi d^2}{\delta} \sin^2\left(\frac{\rho}{2}\right) \int_{\nu_{\min}}^{\nu_{\max}} S_{\text{mean}}(\nu) d\nu, \quad (1)$$

where δ is the pulse duty cycle, d is a distance to the pulsar, ρ is the angular radius of the emitting cone, ν_{\min} and ν_{\max} bracket the radio frequency range in which the pulsar is detected, and $S_{\text{mean}}(\nu)$ is the mean flux density measured at a given frequency ν . The pulse duty cycle can be calculated using the so called equivalent width W_{eq} (i.e. the width of a top-hat pulse having the same area and peak flux as the true profile) as $\delta = W_{\text{eq}}/P$. To derive ρ we have to know the geometry of the pulsar emission beam: α - the inclination angle between the rotation and magnetic axes, β - the impact parameter, and W - the observed pulse width. These values are usually not known for most pulsars. In order to keep the sample of pulsars as large as possible, in this paper we calculate the luminosity L assuming some typical values for all pulsars: $\delta \approx 0.04$, $\rho \approx 6^\circ$, $\nu_{\min} \approx 10^7$ Hz, $\nu_{\max} \approx 10^{11}$ Hz (see Lorimer et al. 2004, for more details), so that

$$L \simeq 7.4 \times 10^{27} \left(\frac{d}{\text{kpc}}\right)^2 \left(\frac{S_{1400}}{\text{mJy}}\right) \text{ erg s}^{-1}. \quad (2)$$

¹ Kepler Institute of Astronomy, University of Zielona Góra, Lubuska 2, 65-265 Zielona Góra, Poland, aszary@astro.ia.uz.zgora.pl

² School of Physics and Kavli Institute for Astronomy and Astrophysics, Peking University, Beijing 100871, China

³ Department of Physics and Astronomy, University of Nevada Las Vegas, NV 89154, USA, zhang@physics.unlv.edu

⁴ Abastumani Astrophysical Observatory, Ilia State University, 3-5 Cholakashvili Ave., Tbilisi, 0160, Georgia

⁵ If not stated otherwise, data presented in this paper are taken from ATNF Pulsar Catalogue <http://www.atnf.csiro.au/research/pulsar/psrcat> (Manchester et al. 2005)

Note that here, we neglect any dependence of $\delta^{-1} \sin^2(\rho/2)$ on the spin parameters P and \dot{P} . In this way we avoid any bias in calculation of L and keep our analysis model-independent (see Section 4 for discussion). Additionally, such an approach allows us to compare the obtained results with X-ray and γ -ray observations.

2.2. Monochromatic luminosities

Sometimes it is convenient to use monochromatic luminosities (often also called “pseudoluminosities”)

$$L_\nu \equiv S_\nu d^2, \quad (3)$$

to estimate how luminosity varies in frequency. Here S_ν is the mean flux density measured at different frequencies (e.g. 400 MHz, 1400 MHz and 2000 MHz). Note that L_ν has the similar dependences on S_ν and d as L .

2.3. Radio emission efficiency

The radio emission efficiency of pulsars is defined as the fraction of rotational energy transformed into radio emission, i.e.

$$\xi \equiv \frac{L}{\dot{E}}, \quad (4)$$

where

$$\dot{E} = 4\pi^2 I \dot{P} P^{-3} \simeq 3.95 \times 10^{31} I_{45} \left(\frac{\dot{P}}{10^{-15}} \right) \left(\frac{P}{s} \right)^{-3} \text{ erg s}^{-1} \quad (5)$$

is the rate of loss of rotational energy (also called spin-down luminosity), and $I = 10^{45} I_{45} \text{ g cm}^2$ is the moment of inertia.

Note that L and \dot{E} are two independent parameters that come from very different measurements. While L is derived from measuring both radio emission flux and distance of a pulsar, \dot{E} is derived from pulsar timing measurements. The L parameter depends on the unknown pulsar radio emission physics. There is no *a priori* reason to expect that ξ should depend on \dot{E} (or other parameters defined by timing parameters) in any way.

3. CORRELATIONS

In the following, we investigate how L and ξ are correlated with other pulsar parameters.

3.1. Spin-down

Figure 1a shows radio luminosity L as a function of the spin-down power \dot{E} . One immediately sees that there is essentially no dependence between the two parameters, with best fit $L \propto \dot{E}^{0.10}$ and $L \propto \dot{E}^{0.06}$ for normal and binary/millisecond pulsars, respectively. A similar conclusion is achieved when one replaces L by pseudoluminosities L_ν . The linear fits in different frequencies show that the exponents for $L_\nu - \dot{E}$ relations are all close to 0, i.e. 0.18, 0.1 and -0.08 for 400, 1400, and 2000 MHz, respectively, with a rough trend that the exponent decreases with increasing frequency. Note, however, the pulsar samples at 400 MHz (641 objects) and especially at 2000 MHz (27 objects) are considerably smaller than that at 1400 MHz (1436 objects).

The weak dependence of L on \dot{E} suggests a near linear inverse correlation between ξ and \dot{E} . Figure 1b shows such an anti-correlation, with the best linear fits $\xi \propto \dot{E}^{-0.90}$ and $\xi \propto \dot{E}^{-0.94}$ for normal pulsars and binary/millisecond pulsars, respectively. Even though the spread in values of both radio luminosity and efficiency is high for a given spin-down luminosity, the $\xi - \dot{E}$ dependence is clearly visible, with low efficiency (e.g. $\xi = 10^{-8} - 10^{-5}$) at high spin-down rate (e.g. $\dot{E} = 10^{36} \text{ erg s}^{-1}$) and high efficiency (e.g. $\xi \gtrsim 10^{-3}$) at low spin-down rate (e.g. $\dot{E} = 10^{30} \text{ erg s}^{-1}$).

Such a near linear inverse correlation between ξ and \dot{E} is non-trivial. For comparison, in panels (c) and (d) in Figure 1 we also show how X-ray and γ -ray efficiencies depend on \dot{E} . It is clearly seen that the X-ray efficiency is essentially independent on \dot{E} , i.e. $\xi_x \propto \dot{E}^{-0.08}$ (see Figure 1c), and the γ -ray efficiency only weakly depends on \dot{E} , i.e. $\xi_\gamma \propto \dot{E}^{-0.5}$ for normal pulsars and as $\xi_\gamma \propto \dot{E}^{-0.24}$ for millisecond ones (see Figure 1d). When calculating both the X-ray and γ -ray efficiencies, we have assumed a same solid angle for all pulsars, which is the same assumption made in calculating radio emission efficiencies.

3.2. Age

From the very beginning of pulsar astronomy it was suggested that radio luminosity of pulsars must decline with age. Such an evolution could explain the rapid drop in pulsar distribution around the period of 1s (Gunn & Ostriker 1970). As suggested by Taylor & Manchester (1977) many more pulsars would be observed if the luminosity were constant.

Since $\dot{E} \propto \dot{P} P^{-3}$ and $\tau \propto \dot{P}^{-1} P$, the above negative linear $\xi - \dot{E}$ correlation would be translated to a positive linear $\xi - \tau$ correlation. Figure 2a shows that such a dependence is indeed there, with a best linear fit (for normal pulsars only) $\xi \propto \tau^{1.06}$. Notice that millisecond pulsars are excluded in the analysis, since they have experienced recycling spin-up process, so that their τ is not the characteristic age since birth.

This interesting relation suggests a surprising result that as a pulsar ages, it somehow transforms its spin-down luminosity more efficiently into radiation. Such a relationship is nontrivial, and provides valuable information about the mechanism of radio emission.

Again for comparison, we plot ξ_x and ξ_γ against τ in Fig. 2b and Fig. 2c, respectively. We find unlike radio emission, there is essentially no obvious correlation in X-rays (with $\xi_x \propto \tau^{0.11}$), and there is only a weak and rather scattered correlation in γ -rays (with $\xi_\gamma \propto \tau^{0.63}$). This again suggests that the radio emission mechanism is different from those of high-energy radiation.

3.3. Selection effect?

The lack of pulsars with high-efficiency, high- \dot{E} and young-age pulsars suggest that there is no significant selection effect for the two reported correlations above. One may still suspect that the two correlations in the low- \dot{E} and old-age regime may be affected by an observational selection effect, which is against the detection of low- ξ pulsars due to the sensitivity limit of radio telescopes.

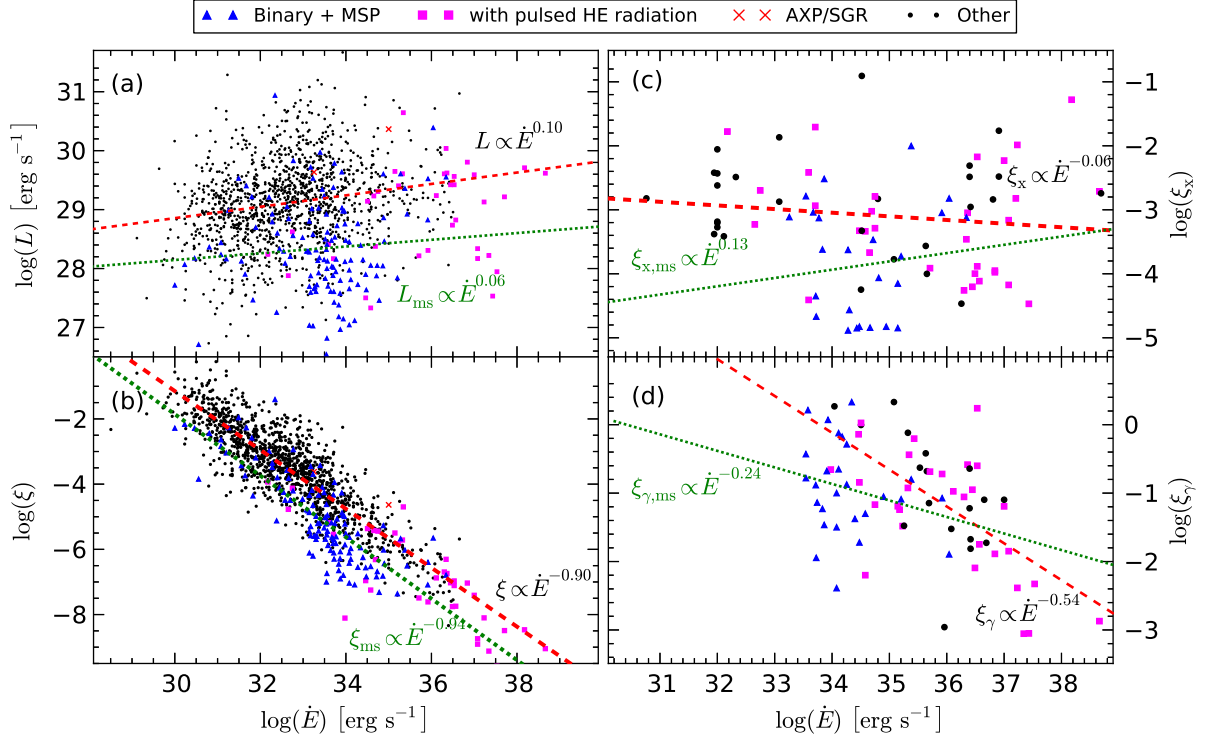


FIG. 1.— Dependence of the radio luminosity L (panel a), and radio (ξ , panel b), X-ray (ξ_x , panel c) and γ -ray (ξ_γ , panel d) efficiencies on the rate of rotational energy losses \dot{E} . The red dashed lines correspond to the linear fit for normal pulsars, while green dashed line represents the linear fit for binary and millisecond pulsars (blue triangles). Pulsars with pulsed high-energetic radiation are marked with magenta squares, whereas anomalous X-ray pulsars (or soft Gamma-ray repeaters) are represented by red crosses. The X-ray data were taken from Szary (2013) for normal pulsars and from Becker (2009) for millisecond pulsars, while the γ -ray data were taken from The Fermi-LAT collaboration (2013).

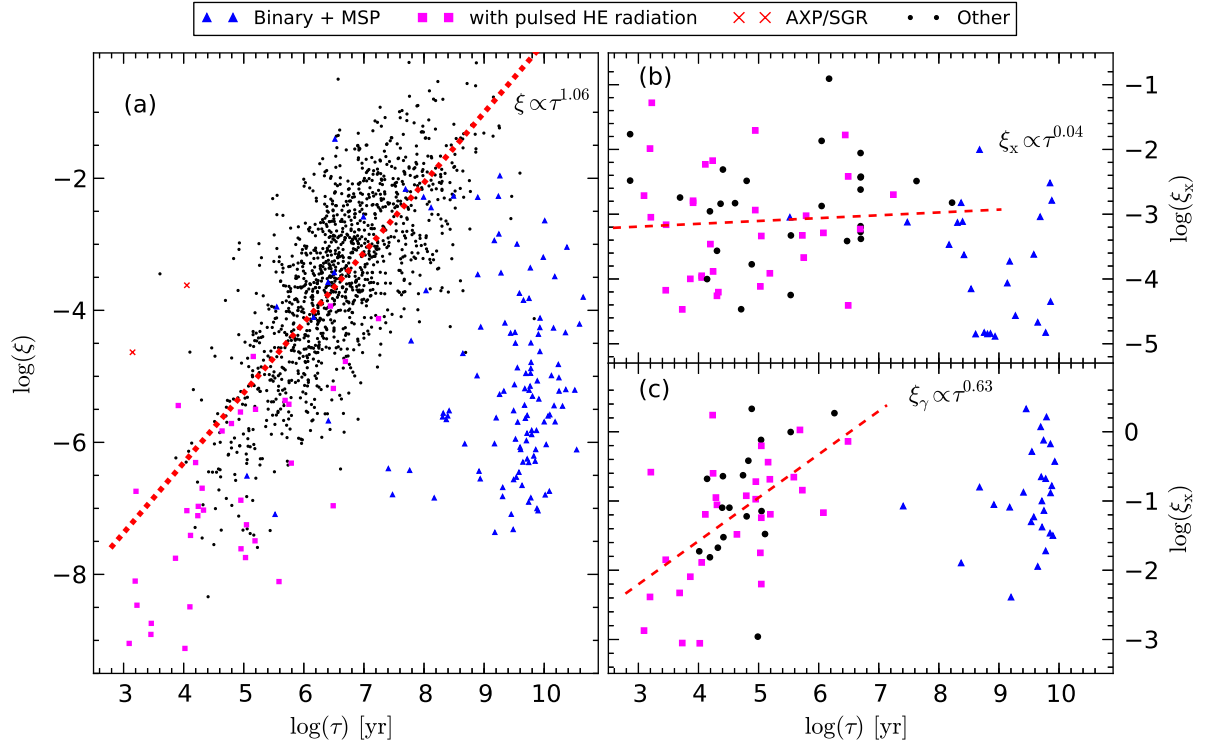


FIG. 2.— Dependence of the radio efficiency ξ (panel a), X-ray efficiency ξ_x (panel b), and γ -ray efficiency ξ_γ (panel c) on pulsar age τ . The dashed lines correspond to the linear fit for normal pulsars. See Figure 1 for more detailed description.

Figure 3 presents the dependence of the observed mean flux density S_{1400} measured at 1400 MHz on the spin-down luminosity \dot{E} . As can be seen from the Figure, the flux distribution of pulsars with relatively low \dot{E} is not significantly different from the flux distribution of pulsars with relatively high \dot{E} . There is no significant depletion of high-flux, low- \dot{E} pulsars, nor an increase of low-flux, low- \dot{E} pulsars. We argue that the relatively large sample of pulsars with $\dot{E} < 10^{31}$ erg/s (143 objects) and the fact that all of them have $\xi > 10^{-4}$ implies that lack of detection of pulsars with low efficiency is not due to insufficient sensitivity of detectors. The two correlations reported above are therefore intrinsic.

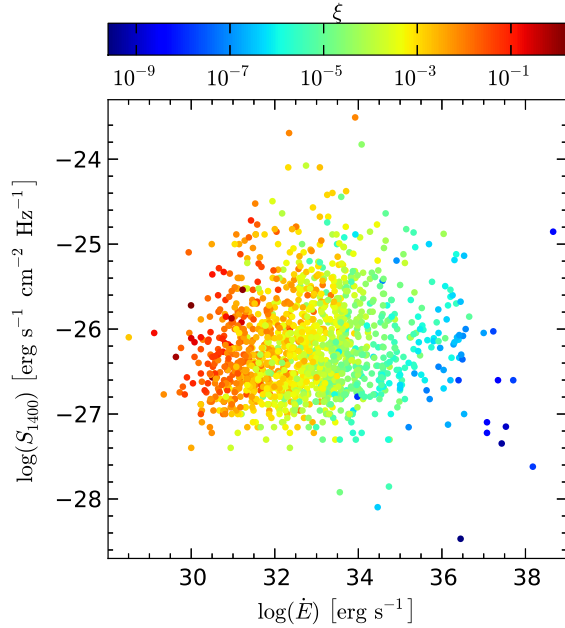


FIG. 3.— Dependence of the observed mean flux density measured at 1400 MHz S_{1400} on spin-down luminosity \dot{E} . Colors correspond to different values of radio efficiency.

3.4. $P - \dot{P}$

There have been efforts to look for how L depends on P and \dot{P} (e.g. Ostriker & Gunn 1969; Lyne et al. 1975; Malov & Malov 2006). The results are affected by the selection effect, and have been inconclusive (see review paper by Bagchi 2013). We will show in this section that these dependences, if any, are rather weak.

We first show the distributions of radio efficiency in different locations of the $P - \dot{P}$ diagram and $P - \tau$ diagram as observed (see Figure 4). As can be clearly seen, the observed radio luminosity does not depend in any significant way on P or \dot{P} .

It would be interesting to investigate the intrinsic underlying P and \dot{P} dependences of L , which may be revealed through Monte Carlo simulations. Faucher-Giguère & Kaspi (2006) (hereafter FK06) argued that in the absence of torque decay (e.g. due to magnetic field decay) the radio luminosity of pulsars must be correlated with pulsar age, and hence

with P and \dot{P} . They found that the luminosity law (i.e. dependence of the radio luminosity on P and \dot{P}) should be close to $L \propto P^{-1.5} \dot{P}^{0.5}$. In order to independently investigate an intrinsic luminosity distribution and eventual dependence of L on P and \dot{P} , we have performed some “Monte Carlo” (MC) simulations based on the open-source package PSRPOP (Bates et al. 2013). This package includes two methods to obtain a synthetic sample of pulsars: the snapshot and evolutionary methods. The snapshot method consists of the following steps: generating pulsar periods, modeling of pulse widths, generating radio luminosities, distributing the pulsars in the Galaxy, modeling electron density, and generating spectral indices. The evolutionary method consists of the steps from the snapshot method but is also extended by additional ones: generating pulsar period derivatives, generating magnetic fields, generating rotational alignment and modeling its time evolution, modeling pulsar spindown, and finally, evolving pulsars through the Galactic potential (see Bates et al. 2013, for more details). Therefore, we used the evolutionary part of this code to reproduce the results of FK06. After the calculation of a synthetic population, each pulsar is run through parameters of the *Parkes Multibeam Pulsar Survey* (Manchester et al. 2001) (PMPS) in order to constrain the population based upon known detections. PMPS is the most successful survey to date with 1062 normal pulsars detected, which allows one to test a synthetic population using more than a half of the total observed population of normal pulsars.

TABLE 1
POPULATION SYNTHESIS PARAMETERS USED IN MC SIMULATIONS
BASED ON THE EVOLUTIONARY METHOD.

Radial distribution model	Yusifov & Kucuk (2004)
R_1	55 pc
a	1.64
b	4.01
Birth height distribution	Exponential
Initial Galactic z-scale height	50 pc
Birth velocity distribution	Exponential
$\langle v_{3D} \rangle$	380 km s $^{-1}$
Pulsar spin-down model	Faucher-Giguère & Kaspi (2006)
Beam alignment model	Orthogonal
Breaking index	3.0
Birth spin period distribution	Normal
$\langle P_0 \rangle$	300 ms a , 200 ms b
σ_{P_0}	150 ms $^a, b$
Scattering model	Bhat et al. (2004)
Spectral index of the scattering model	-3.86
Maximum age of pulsars	1 Gyr
Spectral index distribution model	Normal
$\langle \alpha \rangle$	-1.4
σ_α	0.96
Magnetic field distribution model	Lognormal
$\langle \log_{10} (B_d [\text{G}]) \rangle$	12.65
$\sigma_{\log_{10} B_d}$	0.55
Random luminosity distribution model a	Lognormal
$\langle \log_{10} (L_{1400} [\text{mJy kpc}^2]) \rangle$	-1.1 a , 0.5 b
$\sigma_{\log_{10} L_{1400}}$	0.9 a , 1.0 b
Number of pulsars detected in PMPS	1100

a - population model parameters used to reproduce results of FK06

b - optimal population model parameters

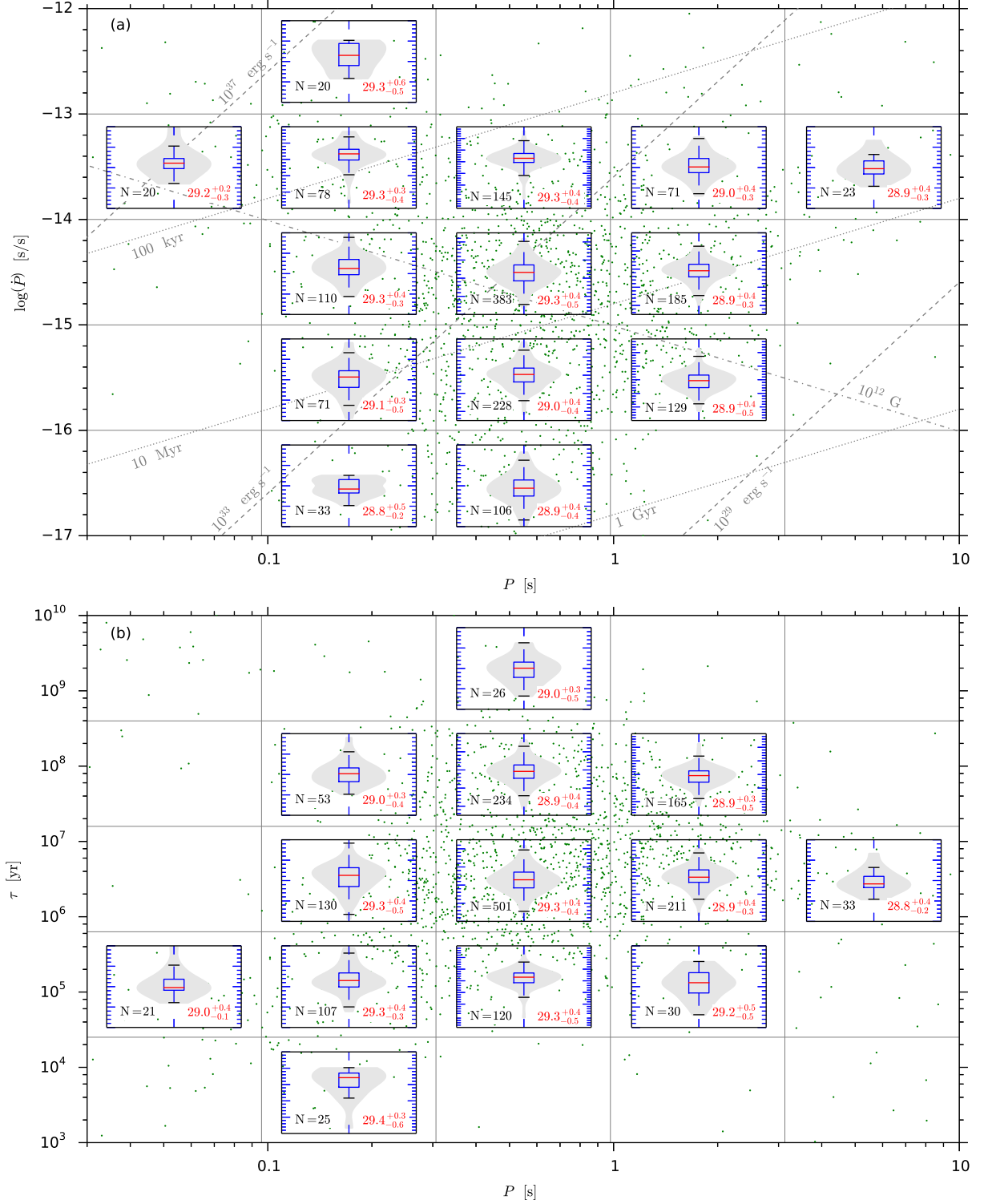


FIG. 4.— Violin histogram plots of pulsar luminosity for the observed sample of pulsars imposed on the $P - \dot{P}$ diagram (panel a) and the $P - \tau$ diagram (panel b). Each histogram is calculated for a sample of pulsars restricted by a corresponding grid (gray solid lines). The red lines correspond to the median values of luminosity. The box plots show interquartile ranges, while the gray shapes represent kernel density estimations. In the panel (a), contours of constant spin-down luminosity, of constant characteristic age and of constant dipolar magnetic field are indicated by dashed, dotted and dot-dashed lines, respectively.

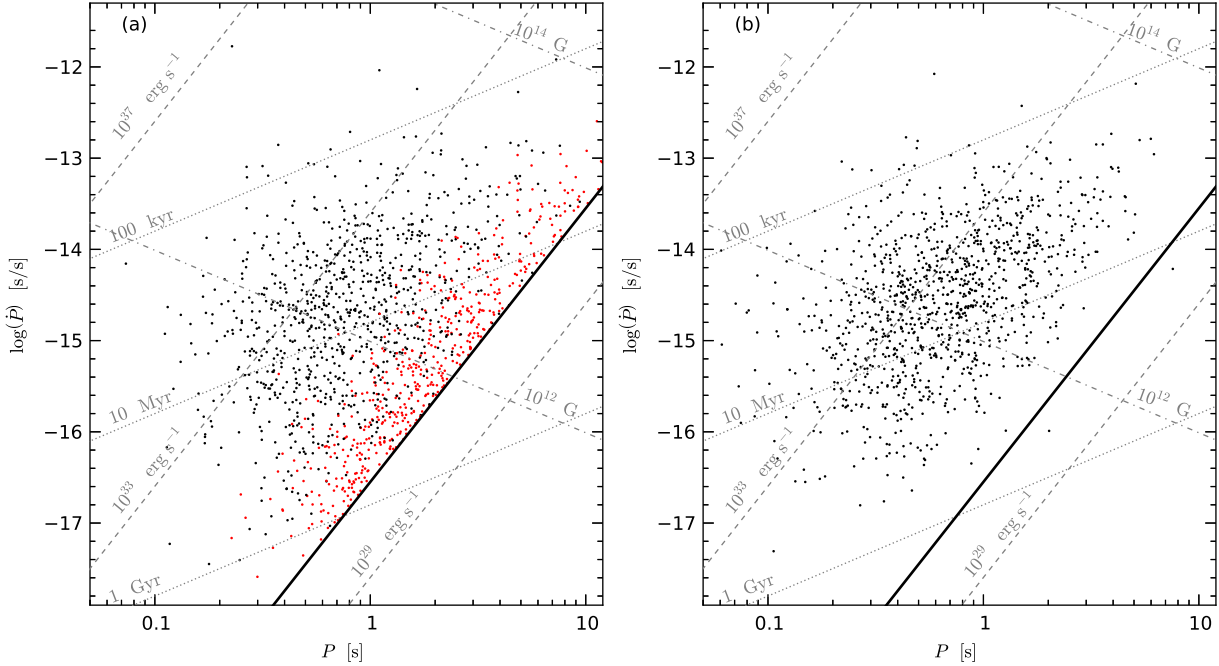


FIG. 5.— $P - \dot{P}$ diagram for a typical MC realization calculated using parameters presented in Table 1 (assuming no magnetic field decay). Contours of constant spin-down luminosity, constant characteristic age and of constant dipolar component of magnetic field are indicated by dashed, dotted and dot-dashed lines, respectively. Red dots correspond to pulsars with radio efficiency greater than one percent. In the panel (a) the thick solid line corresponds to the modeled death line (Bhattacharya et al. 1992), while in the MC realization presented in the panel (b) pulsars were rejected based on the radio efficiency limit $\xi < 0.01$.

Table 1 summarizes the parameters used by FK06 to produce their Figures 7 and 14 calculated, as well as the best fit parameters we have obtained from our simulations (see more details below).

Figure 5a shows the reproduced $P - \dot{P}$ diagram for the random luminosity model calculated using the theoretical death line approximated by the equation $B_d/P^2 = 0.17 \times 10^{12} \text{ G s}^{-2}$ (Bhattacharya et al. 1992) (Figure 14 in FK06). The result is similar to FK06, who noted that, in the absence of magnetic field decay and using the random luminosity model, the results of Monte Carlo-based population synthesis showed a clear pileup of observed objects near the death line in the $P - \dot{P}$ diagram. However, we note that the used approach did not take into account that a radio emission process (whatever it may be) should have an upper limit for its efficiency. In Figure 5a pulsars with derived radio efficiency greater than one percent are marked by red dots. The efficiency of some of these pulsars approaches, and even exceeds 100%. This is physically unreasonable. More likely, the condition for pulsar radio emission may be such that a certain maximum efficiency is imposed. One should check whether the radio efficiency (see Equations 4 and 2) does not exceed 100% ($\xi < 1$) for each independent draw of L_{1400} , P and B_d .

In Figure 5b we show the $P - \dot{P}$ diagram obtained by MC simulation using our optimal random luminosity model (see Table 1) with the condition for pulsar death based only on the upper limit for radio efficiency $\xi_{\text{max}} = 0.01$. Using the efficiency limit allows not only to avoid a pileup of pulsars near the theoretical death line, but also explains the existence of a few pulsars observed in the so-called graveyard region.

In Figure 6 we present comparison of the observed distribution with synthetic distributions for our optimal model (presented in Figure 5b). We have found that the random luminosity model with proper input parameters can reproduce the observed sample much better than the models proposed by FK06. The Kolmogorov-Smirnov (K-S) test on the flux distribution for the power-law model gives the probability (the K-S P-value) 10^{-8} (see Figure 6 in FK06), while the K-S test on the flux distribution for our optimal random luminosity model result in probability of 1%. Note that in our optimal model the distribution of the spin period at pulsar birth is centered at 200 ms. This allowed to obtain the higher probability of reproducing the period distribution than the one obtained by FK06 (compare 4% with 0.7%), but negatively affected the probability of reproducing the period derivative distribution (0.1%), and hence, the B_d distribution (compare 2% with 15%). It is worth noting that one of the parameters which strongly affects both period and period derivative distributions is the maximum efficiency limit. Taking into account a relatively large number of parameters required by the evolutionary method and the fact that we arbitrary choose $\xi_{\text{max}} = 0.01$, the parameters of the model can be further optimized in order to better reproduce the observed sample. Calculations show that using the condition for pulsar death based on the radio efficiency limit allows to avoid pile up of pulsars near the death line. As a result we have found that neither the magnetic field decay nor the dependence of the luminosity on P and \dot{P} are required to reproduce the observed sample⁶.

⁶ This does not mean that the magnetic field decay is not signif-

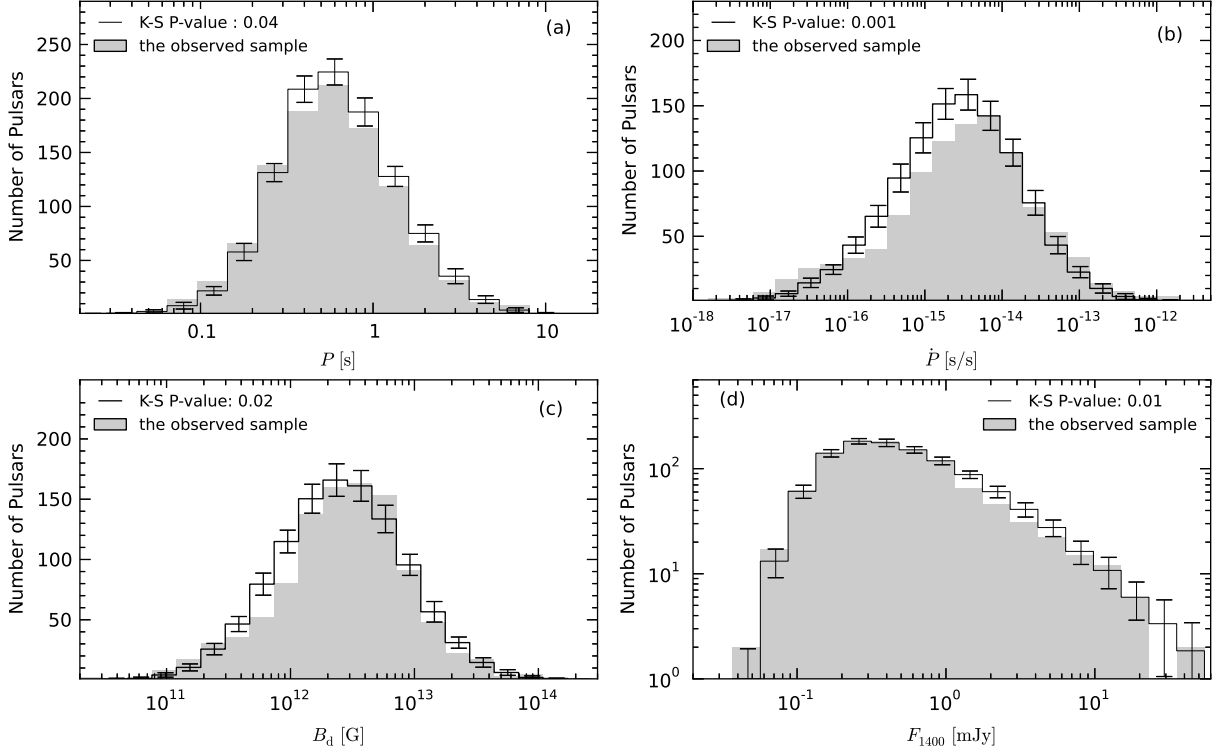


FIG. 6.— Distributions of pulse periods (panel a), period derivatives (panel b), dipolar components of magnetic field at the polar cap (panel c) and radio flux (panel d) compared to the real distributions (filled gray histograms). Distributions correspond to MC simulations using the optimal random luminosity model (see Table 1). For histograms of synthetic data, the number of pulsars in each bin is the average over 50 MC realizations and the error bars indicate the corresponding standard deviations. On each histogram, the corresponding probability from the K-S test is displayed in the legend. All MC pulsars (50×1100) were used to perform the K-S tests.

Figure 7 presents the $P - \dot{P}$ diagram for the whole sample of observed pulsars studied in this paper, with the color scheme denoting how radio efficiency ξ is distributed. The figure clearly shows that the radio emission graveyard in the $P - \dot{P}$ diagram corresponds to a region that ξ may exceed its upper limit (a few percent).

4. SUMMARY AND DISCUSSION

Using a large sample of pulsars from the ATNF catalog, we draw the following conclusions in this paper:

1. Radio pulsar luminosity has a very weak, if any, dependence on pulsar spin-down luminosity \dot{E} over near 8 orders of magnitude in \dot{E} . There might be a slight variation of the exponent of the $L - \dot{E}$ correlation with frequency.
2. There is a near linear inverse correlation between radio efficiency ξ and \dot{E} for both normal and binary/millisecond pulsars.
3. The radio efficiency ξ is roughly linearly correlated with pulsar age τ for normal

icant over lifetime of pulsars as radio-loud sources. We note that even if there is a significant decay of the magnetic field it should be related to a change of the global (dipolar) magnetic field. On the other hand, the existence of non-dipolar configuration of the surface magnetic field was postulated since the very beginning of radio astronomy (Ruderman & Sutherland 1975). We believe that parameters of the plasma (which is responsible for radio emission) strongly depend on the curvature and strength of surface magnetic field. The fact that radio luminosity does not depend in any significant way on the dipolar component of magnetic field (B_d) is a strong proof that the magnetic field at stellar surface is dominated by crust-anchored local magnetic anomalies (see Section 4 for more details).

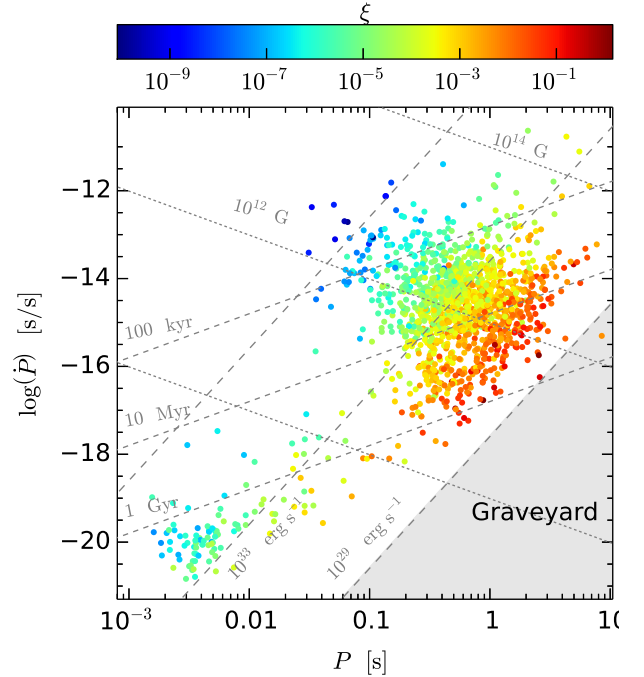


FIG. 7.— The $P - \dot{P}$ diagram shown for a sample 1436 pulsars used in the analysis of radio efficiency. Colors correspond to different values of radio efficiency.

pulsars. 4. The two reported correlations are not due to an observational selection effect. 5. Since radio lumi-

nosity does not depend on P and \dot{P} (or the dependence is very weak) the proposed mechanism of radio emission must explain the significant increase of radio efficiency for low- \dot{E} pulsars.

A weak $L - \dot{E}$ correlation was hinted by previous studies (e.g. Lorimer et al. 1993; Ridley & Lorimer 2010). Malov & Malov (2006) found a weak positive dependence $L \propto \dot{E}^{0.29}$ with a smaller sample (338 objects), which was selected by requiring the pulsars to have well-determined spectra, and/or well-determined distance. We adopt a much larger sample, which has the following advantages. First, a larger sample size can insure more reliable correlations. Second, many uncertainties, e.g. unknown moment of inertia of neutron stars, the influence of scintillation on pulsar flux density, or how well the one-dimensional line-of-sight cut through an emission beam could represent the entire beam, can be effectively canceled out. With our enlarged sample, the index of the correlation, if any, is much flatter than the ones found in the previous studies (see e.g. Arzoumanian et al. 2002; Malov & Malov 2006).

As discussed in §2.1, by using the simplified formula (2), we have neglected some complicated pulsar geometry factors, such as α , β (which defines the duty cycle δ along with P , and ρ). For individual pulsars, the derived L should have a large error. Including the entire sample would cancel out most of these geometric factors, so that our discovered $\xi - \dot{E}$ and $\xi - \tau$ correlations would be intrinsic. One possible factor that is not fully canceled is the P -dependence. This is because both ρ and δ depend on P . However, the explicit exponent of P -dependence is unknown. If we assume that the mechanism of radio emission is the same for both normal and millisecond pulsars, we find that by adding a dependence of $\sim P^{-0.5}$ to the integrated luminosity, the $\xi - \dot{E}$ correlations for both normal and binary/millisecond pulsars become consistent with each other. Adding this period dependence results in the following luminosity relationships: $L_{400} \propto \dot{E}^{0.27}$, $L_{1400} \propto \dot{E}^{0.19}$, $L_{2000} \propto \dot{E}^0$. The found correlations are closer but still shallower than the one found by Malov & Malov (2006). With such a correction, the $\xi - \dot{E}$ correlation is slightly shallower, i.e. $\xi \propto \dot{E}^{-0.81}$, but is still very significant. It has an even lesser impact on the $\xi - \tau$ correlation, i.e. $\xi \propto \tau^{1.01}$ after correction. In a more general form, we can write that $\delta^{-1} \sin^2(\rho/2) \propto P^p \dot{P}^q$. Since in our analysis we are not using geometry information we cannot unambiguously define both p and q . However, assuming similar radio luminosity of normal and millisecond pulsars we can write that $\delta^{-1} \sin^2(\rho/2) \propto P^p \dot{P}^{-0.16(2p+1)}$. Note that even introducing some model-dependent value of p does not change the general picture presented in this paper.

It would seem natural to assume that the spin-down parameters affect the radio luminosity (and hence the radio efficiency) of pulsars. Therefore, many authors (e.g. Ostriker & Gunn 1969; Lyne et al. 1975; Stollman 1986; Malov & Malov 2006; Faucher-Giguère & Kaspi 2006) tried to define the luminosity law, however, the results vary greatly (depending on pulsar samples and used methods) and were inconclusive (see e.g. Bagchi 2013). The spin-down parameters determine the magnetic field strength at the light cylinder

der $B_{LC} \propto P^{-2.5} \dot{P}^{0.5}$. Then, assuming dipolar configuration of magnetic field we can estimate the field strength at the stellar surface as $B_d \propto (P\dot{P})^{0.5}$ and the vacuum potential drop as $V \propto B_d P^{-1} \propto P^{-0.5} \dot{P}^{0.5}$ (Ruderman & Sutherland 1975). The main parameters that affects properties of pulsar radio emission are density and distribution of the electron-positron pair plasma. To estimate the plasma properties we need to use some specific model of acceleration (e.g. the vacuum gap, the space-charged limited flow, the partially screened gap models) and also to take into account various emission processes (e.g. curvature radiation, inverse Compton scattering). It was shown (see e.g. Zhang & Harding 2000; Hibschan & Arons 2001a,b) that the plasma density and distribution highly depend on some factors which cannot be estimated by the spin-down parameters. Thus, we cannot specify the properties of plasma responsible for radio emission using only P and \dot{P} . However, assuming dipolar configuration of pulsar magnetic field, some theoretical predictions suggest that the older the pulsar, the smaller the final pair multiplicity (Hibschan & Arons 2001a,b). It would suggest that some kind of dependence of the radio luminosity on the pulsar age could also be found. As we have shown it is not the case for the observed sample of radio pulsars (see Figure 4).

In order to reproduce the observed sample of pulsars FK06 argued that in the absence of torque decay pulsar radio luminosity has to depend on P and \dot{P} as $L \propto P^{-1.5} \dot{P}^{0.5}$ (or $L \propto P^{-1.39} \dot{P}^{0.48}$ with exponents optimized by Bates et al. (2013)). However, the power-law luminosity model results in relatively low P-value of the K-S test for the flux distribution. We have found that replacing the modeled death line (Bhattacharya et al. 1992) by the radio efficiency limit allows to reproduce the observed sample even with the luminosity model previously excluded by FK06, namely the random luminosity model. Introducing the radio efficiency limit into MC simulations results in much higher probabilities from the K-S test, allows to avoid a pileup of pulsars near the theoretical death line and, furthermore, explains the existence of a few pulsars observed in the so-called graveyard region. We argue that the facts that the observed luminosity does not depend on both P and \dot{P} , and that the random luminosity model of the intrinsic luminosity allows to reproduce the observed sample is a strong indication in favor of the random model.

It is very difficult to explain the spread of up to four orders of magnitude for both L and ξ for a given spin-down luminosity only by statistical uncertainties. As we have mentioned above there must be some parameter/parameters other than P , \dot{P} that influence the radio efficiency of pulsars. The clear $\xi - \dot{E}$ linear inverse correlation and $\xi - \tau$ linear correlation for radio emission call for the following physical picture: The plasma responsible for generating pulsar radio emission must be produced under similar conditions regardless of pulsar age, dipolar magnetic field strength, and spin down rate. One possibility is that the pulsar polar cap region may have dominant crust-anchored magnetic anomalies, so that the near surface magnetic field configuration significantly deviates from the dipolar geometry (Gil et al.

2002a). X-ray observations of old pulsars indeed revealed hot spots that are significantly smaller than the conventional polar cap (Zhang et al. 2005; Gil et al. 2008; Szary 2013), which is consistent with having strong non-dipolar magnetic field at the surface due to crust-anchored local anomalies.

The crust-anchored anomalies can be characterized by a parameter $b = B_s/B_d = A_{dp}/A_{bb}$, which describes the ratio of the actual value of the magnetic field at the surface B_s to the dipolar component of the magnetic field B_d (see e.g. Gil et al. 2002b). Here $A_{dp} \approx 6.2 \times 10^4 P^{-1} \text{ m}^2$ is the conventional polar cap area (i.e. calculated assuming pure dipolar configuration of the magnetic field), and A_{bb} is the actual hot spot area (i.e. derived from X-ray observations). The sample of pulsars with an X-ray hot spot for which b can be estimated is small. Nevertheless, with this small sample (Szary 2013), we can clearly see a correlation between pulsar age and b (see Figure 8).

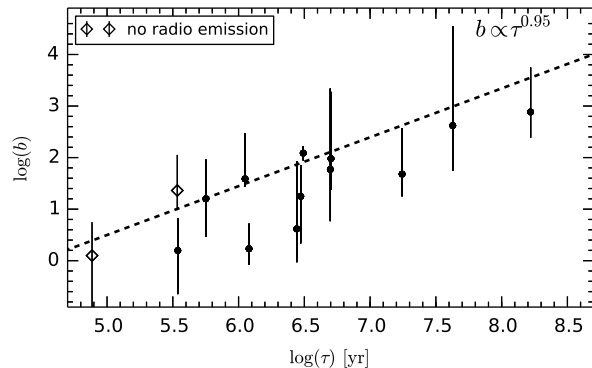


FIG. 8.— Dependence of the b parameter on pulsar age τ (see text for more details). Dashed line correspond to the linear fit for all pulsars with detected radio emission. Note that for PSR J0108-1431 we used the single blackbody fit performed by Pavlov et al. (2009).

The found correlation indicates that when a pulsar be-

comes older, its surface magnetic field becomes more dominated by the crust-anchored magnetic anomalies generated e.g. by the Hall drift (see Geppert et al. 2013; Viganò et al. 2013). Such a crust-anchored anomaly does not depend on \dot{E} and age, which allows pulsars to produce enough electron-positron pairs at an old age to power radio emission.

The fact that pulsars near the graveyard tend to have a very high ξ also has a profound implications in understanding radio pulsar death. Traditionally, pulsar death line (Ruderman & Sutherland 1975; Chen & Ruderman 1993) was defined by the condition of production of electron-positron pairs, which depends on many uncertainties, including the near-surface γ -ray emission mechanism (Zhang et al. 2000) and the magnetic field configurations (Gil & Mitra 2001). The results presented in this paper offer a simpler interpretation to radio pulsar death. It is possible that the required physical condition to power radio emission is similar among pulsars in all ages, which requires a certain minimum spin-down power. When pulsars spin down slightly below this threshold, the radio emission mechanism simply cannot operate. This explains why high ξ pulsars are located near the death line. A similar conclusion was drawn by Arzoumanian et al. (2002) based on modelling “of the birth properties and rotational, kinematic, and luminosity evolution of a Monte Carlo population of neutron stars”, even though the luminosity and spin-down rate scaling presented in their work, $L \propto \dot{E}^{0.5}$, does not reflect the actual $L - \dot{E}$ relationship (see Figure 1a).

This work is partially supported by a visitor program of Kavli Institute for Astronomy and Astrophysics, Peking University, China, and National Science Centre Poland under grants 2011/03/N/ST9/00669 and DEC-2012/05/B/ST9/03924. B.Z. acknowledges NASA NNX10AD48G for support, and R.X.X. acknowledges support by the National Science Foundation of China under Grant No. 11225314. We thank the anonymous referee for constructive comments.

REFERENCES

- Arons, J. 1996, *A&AS*, 120, 49
 Arzoumanian, Z., Chernoff, D. F., & Cordes, J. M. 2002, *ApJ*, 568, 289
 Bagchi, M. 2013, arXiv:1306.2152
 Bates, S., Lorimer, D., Rane, A., & Swiggum, J. 2013, arXiv:1311.3427
 Becker, W. 2009, *Astrophysics and Space Science Library*, 357, 91
 Bhat, N. D. R., Cordes, J. M., Camilo, F., Nice, D. J., & Lorimer, D. R. 2004, *ApJ*, 605, 759
 Bhattacharya, D., Wijers, R. A. M. J., Hartman, J. W., & Verbunt, F. 1992, *A&A*, 254, 198
 Chen, K., & Ruderman, M. 1993, *ApJ*, 402, 264
 Contopoulos, I., & Spitkovsky, A. 2006, *ApJ*, 643, 1139
 Faucher-Giguère, C.-A., & Kaspi, V. M. 2006, *ApJ*, 643, 332, FK06
 Geppert, U., Gil, J., & Melikidze, G. 2013, *MNRAS*, 435, 3262
 Gil, J., & Mitra, D. 2001, *ApJ*, 550, 383
 Gil, J. A., Melikidze, G. I., & Mitra, D. 2002a, *A&A*, 388, 235
 Gil, J. A., Melikidze, G. I., & Mitra, D. 2002b, *A&A*, 388, 246
 Gil, J. A. et al. 2008, *ApJ*, 686, 497
 Gunn, J. E., & Ostriker, J. P. 1970, *ApJ*, 160, 979
 Hirschman, J. A., & Arons, J. 2001a, *ApJ*, 560, 871
 Hirschman, J. A., & Arons, J. 2001b, *ApJ*, 554, 624
 Lorimer, D. R., Bailes, M., Dewey, R. J., & Harrison, P. A. 1993, *MNRAS*, 263, 403
 Lorimer, D. R., Kramer, M., Ellis, R., et al. 2004, *Handbook of pulsar astronomy*, by D.R. Lorimer and M. Kramer. Cambridge observing handbooks for research astronomers, Vol. 4. Cambridge, UK: Cambridge University Press, 2004,
 Lorimer, D. R., Faulkner, A. J., Lyne, A. G., et al. 2006, *MNRAS*, 372, 777
 Lyne, A. G., Ritchings, R. T., & Smith, F. G. 1975, *MNRAS*, 171, 579
 Malov, I. F., & Malov, O. I. 2006, *Astronomy Reports*, 50, 483
 Malov, I. F., & Malov, O. I. 2007, *VizieR Online Data Catalog*, 908, 30542
 Manchester, R. N., Hobbs, G. B., Teoh, A., & Hobbs, M. 2005, *AJ*, 129, 1993
 Manchester, R. N., Lyne, A. G., Camilo, F., et al. 2001, *MNRAS*, 328, 17
 Mastrano, A., Lasky, P. D., & Melatos, A. 2013, arXiv:1306.4503
 Melrose, D. B. 2006, *Chinese Journal of Astronomy and Astrophysics Supplement*, 6, 020000
 Ostriker, J. P., & Gunn, J. E. 1969, *Nature*, 223, 813
 Pavlov, G. G., Kargaltsev, O., Wong, J. A., & Garmire, G. P. 2009, *ApJ*, 691, 458
 Ridley, J. P., & Lorimer, D. R. 2010, *MNRAS*, 404, 1081

- Ruderman, M. A., & Sutherland, P. G. 1975, ApJ, 196, 51
Stollman, G. M. 1986, A&A, 170, 48
Szary, A. 2013, arXiv:1304.4203, PhD Thesis
Taylor, J. H., & Manchester, R. N. 1977, ApJ, 215, 885
The Fermi-LAT collaboration 2013, arXiv:1305.4385
Viganò, D., Rea, N., Pons, J. A., et al. 2013, MNRAS, 434, 123
Yusifov, I., Kucuk, I. 2004, A&A, 422, 545
Zhang, B., & Harding, A. K. 2000, ApJ, 532, 1150
Zhang, B., Harding, A. K., & Muslimov, A. G. 2000, ApJ, 531, L135
Zhang, B., Sanwal, D., & Pavlov, G. G. 2005, ApJ, 624, L109